Journal of King Saud University – Science 32 (2020) 1346–1352

Contents lists available at ScienceDirect

Journal of King Saud University – Science

journal homepage: www.sciencedirect.com

Original article

Green synthesis of silver nanoparticles from *Neurada procumbens* and its antibacterial activity against multi-drug resistant microbial pathogens

Fahad A. Alharbi *, Abdullah A. Alarfaj

Department of Botany and Microbiology, College of Science, King Saud University, PO Box 4255, Riyadh 11451, Saudi Arabia

ARTICLE INFO

Article history:
Received 27 October 2019
Revised 17 November 2019
Accepted 20 November 2019
Available online 27 November 2019

Keywords:
Silver
Nanoparticle
Antibacterial
MDR bacteria
Clinical isolates

ABSTRACT

The aim of this work was to develop a new biological process for the fabrication of silver nanoparticles (Ag-NPs) using the extract of a xerophytic plant (*Neurada procumbens*) as a reducing agent. The fabricated Ag-NPs can effectively control multi-drug resistant gram-negative rods (MDR-GNRs), which were isolated from the Buraidah Central Hospital (BCH), Saudi Arabia. The predominant MDR-GNR bacteria included *Klebsiella pneumoniae, Acinetobacter baumannii,* and *Escherichia coli*. The Ag-NPs were examined by diverse spectral and analytical techniques, and then their antibacterial effects against MDR bacteria were determined. The UV spectroscopy showed absorption peaks between 400 and 455 nm specific to AgNPs. The SEM and TEM results showed a smallsize of Ag-NPs in a range of about 20–50 nm. The XRD pattern showed three major distinctive peaks of Ag-NPs at 38.1°, 44.3° and 64.4° confirming the presence of Ag-NPs. Three multidrug-resistant bacterial strains were used to determine antimicrobial activity by the well-diffusion method. The present workillusrates that synthesized Ag-NPs from the aqueous leaf extract of *Neurada procumbens* show considerable antibacterial potential against MDR clinical isolates from different patient samples at BCH.

© 2019 Published by Elsevier B.V. on behalf of King Saud University. This is an open access article under the CC BY-NC-ND license (http://creativecommons.org/licenses/by-nc-nd/4.0/).

1. Introduction

In the past two decades, public health standards in numerous parts of the world have changed due to the increase in infectious diseases (AlSalhi et al., 2016; Devanesan et al., 2017). The reason is that misuse or overuse of antibiotics for bacterial infections has led to resistance against many antibiotics. The Multidrug Resistance (MDR) pathogens cause additional complications in respiratory and urinary tract infections (Allaker, 2010; Azhaguraja et al., 2017; Devanesan et al., 2018; AlSalhi et al., 2019; Alfuraydi et al., 2019). MDR bacteria is considered to be the greatest threats to public health worldwide and it is often significantly harder to curb (Roca et al., 2015; Al-Dhabi and Ghilan, 2019). MDR in bacteria might be produced by either of the one of the two mechanisms (Al-Dhabi and Ghilan, 2018). Firstly, the bacteria might accumulate several different resistance genes within a single cell (Al-Dhabi et al., 2019) Afterwards, this accumulation arises usually on resistance (R) plasmids. The plasmid might be transported to another cell quickly by means of metabolic process. Since a single plasmid might transport R genes for many drugs, a pathogen population can become resistant to numerous antibiotics instantaneously, although the affected patient is being cured with either one of the antimicrobial agent. General antibiotic cure favors the advancement and spread of antibiotic R strains since the antibiotic destroys the normal bacterial flora that would typically contest with antibiotic R strain. Therefore, MDR in bacteria is controlled by a gene on "R" plasmids or transposons and each gene codes for resistance to a specific agent (Vijayaraghavan et al., 2012) or antibiotic. As a result, each MDR bacterium has its own mechanism of action. Many of the difficulties arise from the misuse and overuse of drugs. However, some physicians administer antibacterial drugs to patients with viral infections such as cold and influenza viral pneumonia (Murugan et al., 2016), and it have been estimated that over 50% of the antibiotics are prescribed without clear evidence of infection. In some cases, antibiotics are prescribed for particular pathogens without bacterial infection and drug sensitivity test report. Using broad-spectrum antibiotics in place of narrow-spectrum ones creates hazardous side effects and increases bacterial resistance capacity. Bacterial R to certain types of antibiotics is a natural phenomenon that occurs by gene mutation and acquiring resistance from other bacteria. Further, the genes for MDR are

* Corresponding author.
E-mail address: fhloon@yahoo.com (F.A. Alharbi).

Peer review under responsibility of King Saud University.

Production and hosting by Elsevier

https://doi.org/10.1016/j.jksus.2019.11.026
1018-3647/© 2019 Published by Elsevier B.V. on behalf of King Saud University.
This is an open access article under the CC BY-NC-ND license (http://creativecommons.org/licenses/by-nc-nd/4.0/).

found in both the bacterial chromosome and plasmid. Bacteria become drug-resistant in numerous ways such as by preventing the entry of the drug. For example, penicillin G cannot penetrate the envelope's outer membrane of numerous Gram-negative bacteria (Link-Gelles et al., 2013). Some pathogens modify their penicillin-binding proteins and create resistance. In addition, reduced permeability might result in a sulfonamide R. Numerous bacterial pathogens create resistance by inactivating drugs by means of surface modification. Dobbins stated that each chemotherapeutic agent is targeted by a specific enzyme or organelle so that were not susceptible to the drug. For instance, the affinity of ribosomes for erythromycin and chloramphenicol can be reduced by the changes in the 23S rRNA to which they bind. *Klebsiella pneumoniae, Escherichia coli*, and *Pseudomonas aeruginosa* have developed resistance against common antibiotics comprising ampicillin, chloramphenicol, kanamycin, tetracycline, and trimethoprim, whereas *Neisseria gonorrhoeae* is resistant to penicillin, tetracycline, and fluoroquinolones (Chang et al., 2015). Recently, nanoparticles have attracted great attention in medical applications owing to the limitation of numerous infectious microorganisms. Generally, the antimicrobial effect of nanoparticle (NPs) appears via the disruption of the bacterial cell membrane, penetration or generation of reactive oxygen species (ROS) by increasing ROS levels, this oxidative stress in the normal redox state of cell can influence toxic effects by means of the creation of peroxides and free radicals that damage all constituents of the bacteria cell, comprising proteins, lipids, and DNA (Panda et al., 2011). There are many studies on the synthesis and characterization of many metallic NPs such as Ag, Cu, Au, Al, Ti, Fe, Zn, Bi, and among others, which are employed as budding antimicrobial agents (Brown et al., 2012). Among the NPs, Ag nanoparicles (Ag-NPs) have been used to fight infections and control spoilage (Arasu et al., 2017; Arasu et al., 2019; Arokiyaraj et al., 2015). Besides, Ag-NPs play a significant part in the clinical field owing to its distinctive physicochemical properties, which include antimicrobial and anticancer effects (Boovaragamoorthy et al., 2019; Gurusamy et al., 2019; Ilavenil et al., 2015). Our study deals with the synthesis of Ag-NPs by reducing Ag ions exist in $AgNO_3$-solution using cell-free aqueous extract of *Neurada procumbens* leaf. The obtained particles were analyzed using UV–Vis spectroscopy, SEM, TEM, and XRD. Besides, the antibacterial nature of the fabricated NPs was examined against the most predominant MDR-GNR bacteria at BCH during January-June 2017.

2. Materials and methods

2.1. Materials

Different xerophytic plants, namely, *Pulicaria undulata*, *Neurada procumbens*, *Citrullus colocynthis*, *Emex spinosa,* and *Chrozophora tinctoria*, were collected from Riyadh, Saudi Arabia. All the healthy plants were brought to the laboratory immediately with utmost care. The collected plants were submitted and analyzed by the Curator Herbarium Unit, Department of Botany and Microbiology, KSU.

2.2. Preparation of leaf extract

All healthy leaves from each plant were hand-picked and washed carefully with normal water and then by distilled water. Fresh plant leaves (20 g) were weighed and cut into fine pieces using a clean stainless steel knife. The leaves were then boiled with 100 mL of water for 10 min in a 250 mL Erlenmeyer flask. The aqueous extract was then separated using Whatman filter paper (150 mm). The filtrate was centrifuged at 1200 rpm for 5 min to remove unwanted cell debris. Finally, the obtained extract was kept at 4 °C for the future analysis.

2.3. Synthesis of Ag-NPs

$AgNO_3$ was used as the preliminary material for the synthesis of Ag-NPs. For the synthesis of 1 mM of $AgNO_3$ solution, about 17 mg of $AgNO_3$ salt was weighed and dissolved in 100 mL of double distilled water and stirred for 10 min. Then it was transferred to an amber-colored bottle and stored in dark at room temperature. Every time a freshly prepared solution was used for avoiding oxidation process (Priya Banerjee and Aniruddha, 2014). Of each extract, 10 mL was mixed with 90 mL of $AgNO_3$ solution, 1/9 of the extract was reduced into Ag^+ ions. In order to optimize the incubation time and temperature, five sets of the above-mentioned mixture were prepared and kept at different temperatures such as room temperature, 35 °C, 50 °C, 75 °C, and 95 °C using water bath incubator, respectively (Ping et al., 2018).

2.4. Characterization of Ag-NPs

The maximum absorption wavelength of the obtained nanoparicles was measured by VU spectrum. The crystalline nature of Ag-NPs was evaluated via X-Ray diffractometer, Rigaku (Ultima IV) instrument. The morphological nature of the Ag-NPs was examined by SEM and TEM analysis. The SEM measurements were carried out using JEOL-Japan Electron Optics Laboratory JSM-6380 LA and the TEM measurements were assessed using JEM-1010.

2.5. Antimicrobial assay

The antimicrobial activity was performed using the agar well diffusion method (Brown et al., 2012; Arasu et al., 2013).

3. Results and discussion

3.1. UV–Vis spectral analysis

Five different desert plant leaves were engaged for the fabrication of Ag-NPs. Of these five plants, *Neurada procumbens* (Fig. 1) gave the most appropriate and effective nanoparticles. The reaction mixture was prepared by mixing plant extracts with $AgNO_3$ (1: 9) and incubated at 35 °C, 50 °C, 75 °C, 85 °C, and 95 °C. The $AgNO_3$ solution without plant extract was considered as control. Fig. 2A

Fig. 1. Micrograph of *Neurada procumbens.*

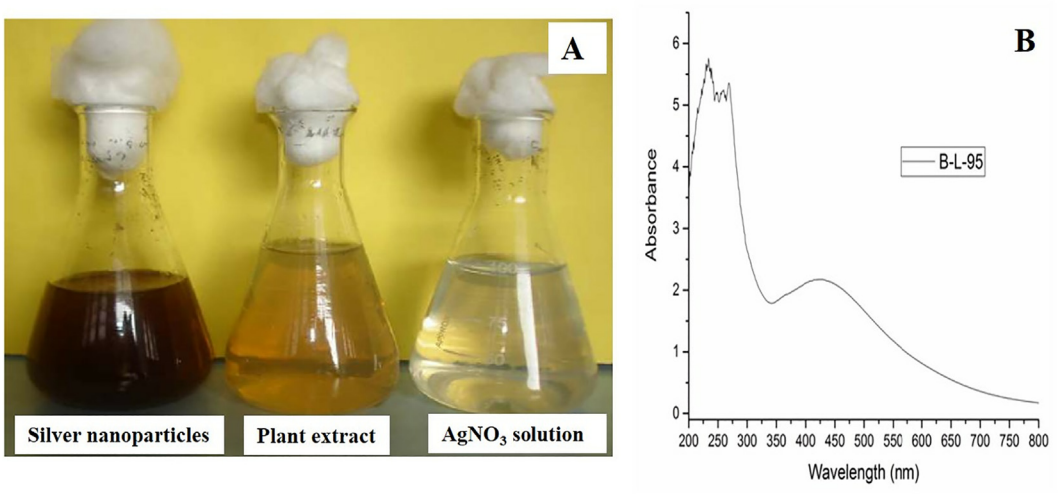

Fig. 2. A) Images of $AgNO_3$ solution, Plant extract and AgNP solution, B) UV–visible spectrum.

shows images of $AgNO_3$, plant extract and Ag-NPs produced. Initially, the reaction mixture of $AgNO_3$ solution and plant extract was start-yellowish color, after incubation at different temperatures; Ag-NPs were seen as yellow to dark brownish color at all temperatures within 15 min. Under normal circumstances, the color change was noticed after 12 h. The color change evidenced the creation of Ag-NPs. The flask was then taken from the incubator and wrapped in Al foil to inhibit light to interact with bare $AgNO_3$ (Kumar et al., 2014; Rajkumari et al., 2019a,b; Roopan et al., 2019).

The formation of NPs was analyzed by means of UV–visible spectrophotometer (Fig. 2B) (Valsalam et al., 2019a). Surface plasmon resonance (SPR) of the synthesized Ag-NPs, appear as peaks due to the characteristic SPR of Ag-NPs. Moreover, the present work confirmed that small-sized Ag-NPs were produced at 95 °C. Kumar et al. (2014) reported that the formation of narrow peaks in the UV spectra indicates the synthesis of small-sized nanoparticles. Further, the average diameter of Ag-NPs increased with the higher reaction mixture (plant extract and $AgNO_3$) leading the Ag^+ ions to completely convert into Ag-NPs with an increased rate of the reaction. The greater intensity might be credited to higher absorption and larger surface area of nanoparticles. Surface electron oscillation is reliant on on the particle size and shape, and hence reflects different colors. The Ag-NPs suspension was kept safely for about one month to examine the long-term nature of the fabricated NPs. After one month, the long-term stability was determined by means of absorption spectra after one month under identical conditions but there was no substantial change in the absorption, which indicated that the NPs are stable for up to one month.

3.2. SEM analysis

SEM was used to assess the morphological nature of Ag-NPs. SEM images showed predominantly spherical-shaped NPs. The maximum size of the nanoparticles was always lower than 100 nm and the average size of green synthesized Ag-NPs was ranging between 20 and 50 nm. SEM results (Fig. 3A-D) confirmed that *Neurada procumbens* leaf extracts may perform as reducing and capping agents for the creation of Ag-NPs effectively. In agreement with our results, spherical and cubic shaped Ag-NPs, with a size ranging from 35 to 65 nm, were synthesized using *Centroceras clavulatum*.

3.3. TEM analysis

TEM analysis revealed spherical-shaped Ag-NPs of size varying from 20 to 40 nm (Fig. 4A-D). Afterwards, the small-sized NPs were created owing to the strong redox reaction between *Neurada procumbens* extract and aqueous Ag metal ions (Valsalam et al., 2019b). The appearance of dark caps on the surface of nanoparticles exhibited the presence of secondary materials. This might be ascribed to bio-molecules existing in the leaf extract. These biomolecules can effect in the effective reduction of Ag salts to NPs and work as suitable capping agent, thereby preventing them from aggregation.****Fig. 5.

3.4. XRD analysis

The green synthesized Ag-NPs were characterized using powder XRD. A representative XRD is based on the constructive interference of monochromatic X-rays and a crystalline information of the materials. The diffraction pattern clearly shows the main peaks at 2 h of annealing, 38.19°, 44.37°, 64.56° and 77.47°, corresponding to the planes 101, 111, 200 and 220, respectively (Fig. 6). Similar results were observed by (Jeeva et al., 2014) who identified crystalline peaks at 32.28, 46.28, 54.83, 67.47 and 76.69, which were also obvious in many other studies in which the XRD pattern involved the significant 2θ range.

Earlier researchers have reported similar results for Ag-NPs (Gopinath et al., 2012). Green synthetic approaches to fabricate the Ag-NPs were recorded by the XRD pattern. The peaks were identified conforming to (*h k l*) values of Ag. Particularly, the XRD measurements evidenced that the subsequent particles are Ag-NPs tends to possess an fcc structure. Further, the average crystalline size D, the assessment of the inter-planar spacing between the atoms, d, lattice constant and cell volume have been assessed. Thus, Ag-NPs with distinct dimensions might be fabricated by plant compounds (Bindhu and Umadevi, 2014).

3.5. Microbial analysis

The well diffusion method was used to assess the antibacterial behaviors of the fabricated Ag-NPs that were assessed against a group of bacteria collectively called MDR-GNR. It is a mixed group of various bacterial species and genera such as *K. pneumoniae, A.*

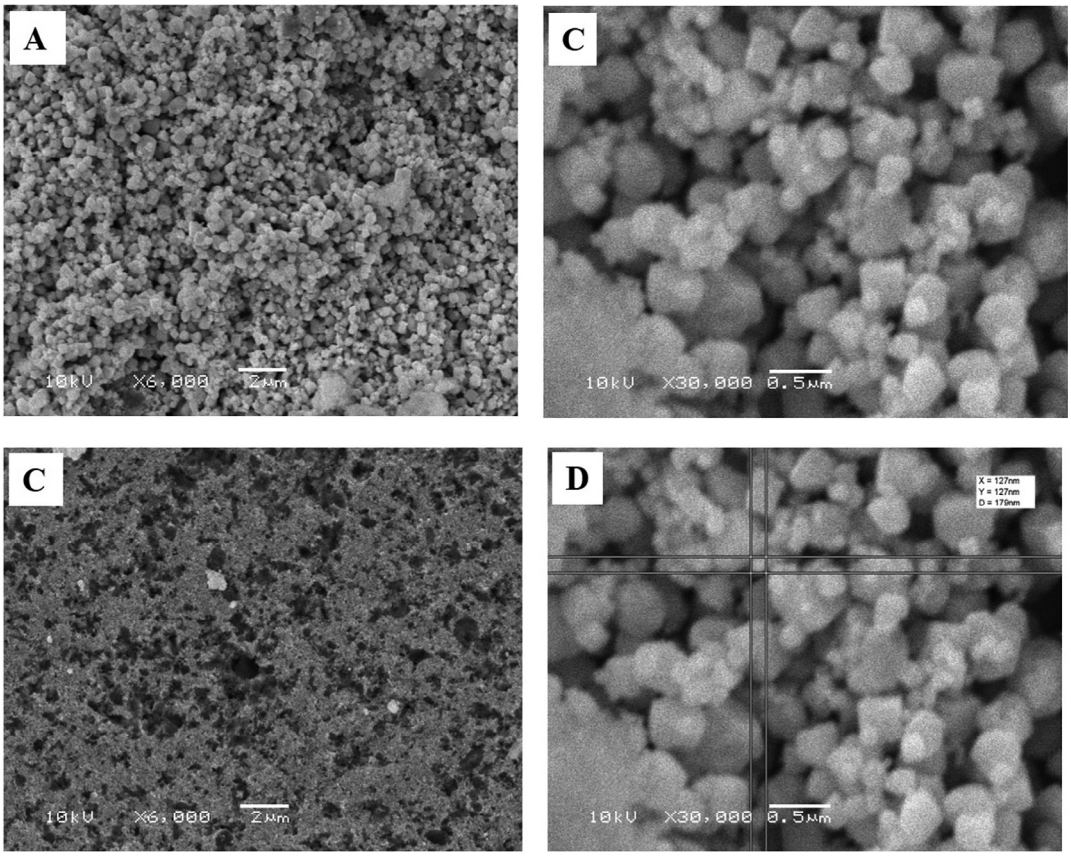

Fig. 3. SEM analysis of the AgNPs.

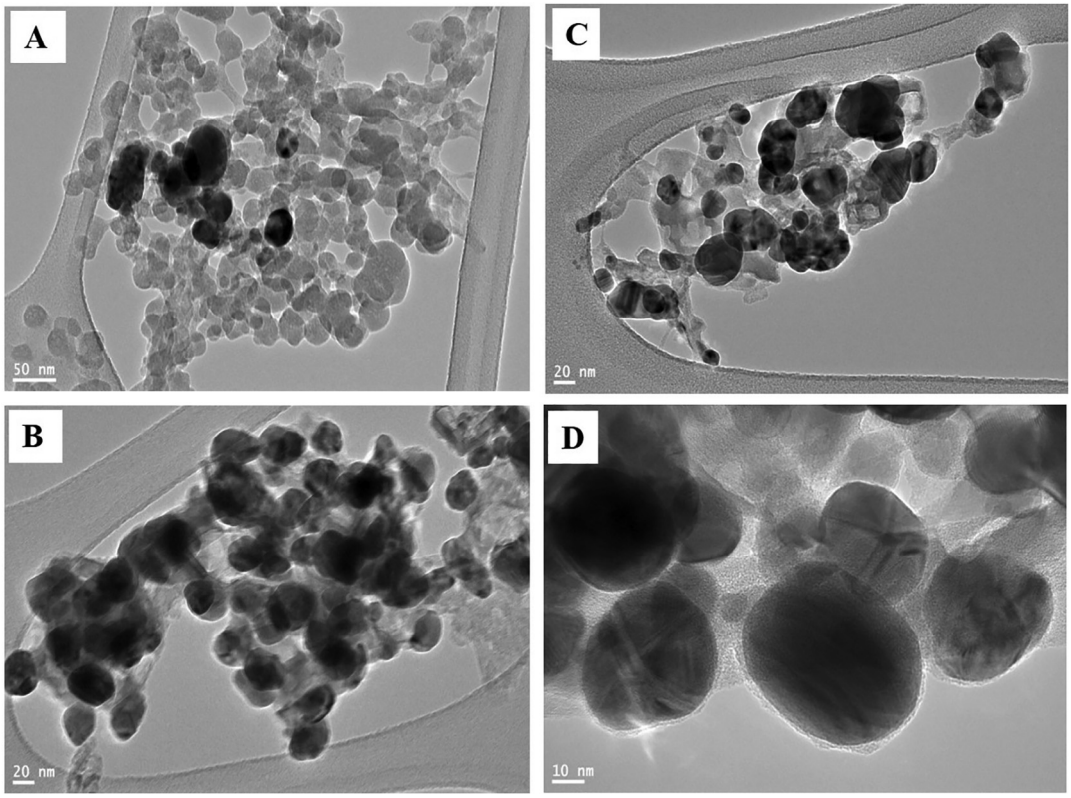

Fig. 4. TEM analysis of the AgNPs.

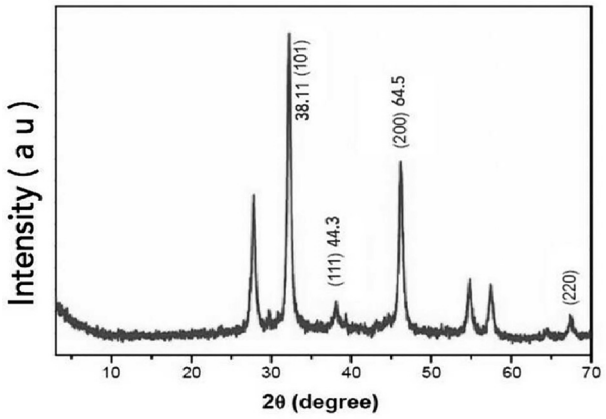

Fig. 5. XRD spectra of the AgNPs.

baumannii, and *E. coli* having resistance to a variety of antibiotics (Table 1).

The loaded Mueller-Hinton (MH) agar plates were incubated at 37 °C for 24 h. Five holes were made in MH agar plate at five different concentrations of Ag-NPs (μg/mL = total volume of 1 mL) 10 μg, 25 μg, 50 μg, 75 μg, and 100 μg. The zone of inhibition was estimated by means of evaluating the diameter of the inhibition zone around Ag-NPs (Fig. 6). When a 6 mm hole was impregnated with Ag-NPs in a MH agar plate, the antimicrobial immediately arises to diffuse into the neighboring agar. Out of the five concentrations (from 10 μg to100 μg) of nanoparticles poured into each well, the microbial growth was decreased with increasing concentrations of nanoparticles.

The sensitivity of *Escherichia coli, Acinetobacter baumannii,*and *Klebsiella pneumoniae* to a range of Ag-NPs100 μg–75 μg as assessed using plate diffusion assay. The experiment was repeated three times (Table 2)

Plant phytochemicals assist in the creation of Ag-NPs (Feng et al., 2000) and from the results, it is obvious that the zone of inhibition upsurges linearly with an increase in the concentration of NPs, which is in consistent with other reports (Valsalam et al., 2019a; Valsalam et al., 2019b) These results indicated that most of the bacteria are resistant to the antibiotics tested manually on MH agar or automated by Microscan.

The present results indicate that Ag-NPs have stronger antibacterial activity against all isolated MDR strains. However, the exact mechanism of the antibacterial activity of Ag NPs is not fully understood. Some researchers reported on the possible mechanisms of Ag-NPs such as interaction of Ag ions and bacteria, electrostatic interaction between positively charged Ag ions with negatively charged DNA and protein (Dibrov et al., 2002) cell membrane and disturbance of membrane permeability (Panacek et al., 2006) the involvement of free radicals of Ag-NPs on membrane damage (Kim et al., 2007), release of lipopolysaccharides from the membrane due to metal depletion in the outer membrane, and the final collapse of the cell. Disruption of ATP production, DNA replication, or cell membrane damage causes the generation

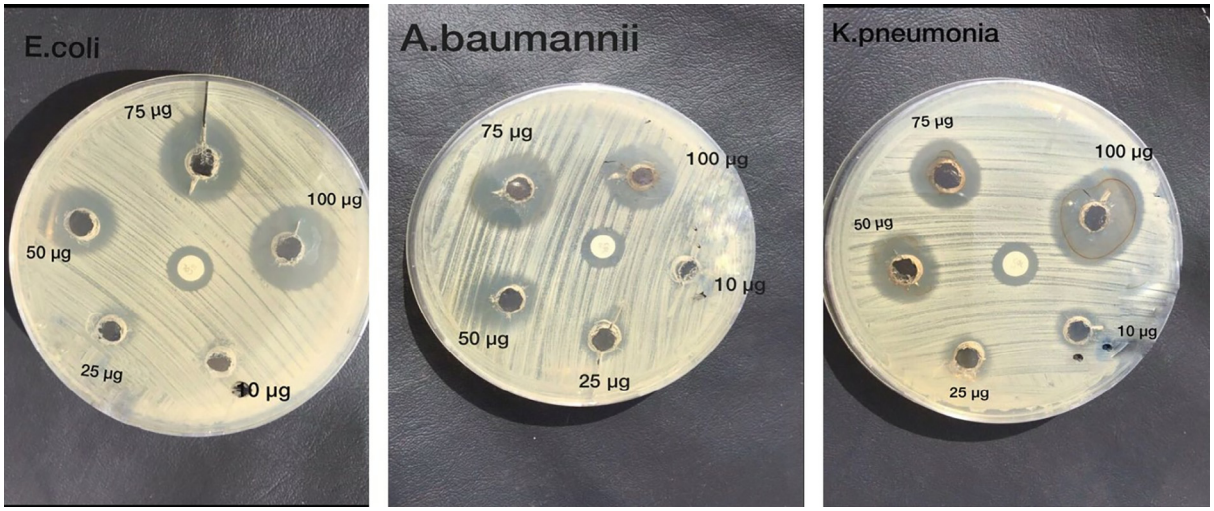

Fig. 6. Antibacterial activity of Ag-NPs against MDR-GNR bacteria.

Table 1
MIC for the MDR-GNR bacteria reported in the BCH patients by Automated MicroScan instrument.

E. coli		*A. baumannii*		*K. pneumoniae*		MDR-GNR Antibiotics
		MIC (minimum inhibitory concentration)				
Su	R	Su	R	Su	R	
–	–		–	–	16/8	Augmentin
	>16		–	–	>16	Ampicillin
≤16	–		>32	–	>32	Amikacin
–	–		–	–	–	Vancomycin
–	–		–		≤8	Cefoxitin
	≥4		>8	–	≤4	Imipenem
<2		<2		<2		Colistin
	>2		>2		>2	Ciprofloxacin
	>8		>8		>8	Gentamicin
	<16		>16		>16	Cefepime
	>8		>8	≤4		Tetracycline

Table 2
Zone of inhibition of Ag-NPs and polymyxin E against MDR-GNR bacteria.

No.	MDR-GNR	Zone of inhibition in mm					
		Colistin 10 μg >14	Concentration of Ag-NPs				
			10 μg	25 μg	50 μg	75 μg	100 μg
1	*K. pneumoniae*	14	R	R	I	I	S
2	*A. baumannii*	14	R	R	I	S	I
3	*E. coli*	14	R	R	I	S	S

S: Sensitive > 17 mm (100 μg,75 μg from Ag-NPs more effective to all strains).
R: Resistant < 14 mm (10 μg, 25 μg from Ag-NPs are resistant to all strains).
I: intermediate 12–14 mm (50 μg from Ag-NPs intermediate to all strain).
Colistin: CLSI interpretive criteria in disc diffusion (≥14 sensitive).

of ROS. Sondi (2004) reported that Ag-NPs at the initial stage of bacterial interaction, adhere to the bacterial cell wall, then penetrate and kill the bacteria (Rajkumari et al., 2019a,b). The higher zone of inhibition for Ag-NPs is affected by the small-sized Ag-NPsthat release diffusible inhibitory compounds.

4. Conclusion

In summary, Ag-NPs were synthesized using the plant extract from *Neurada procumbens* as a reducing agent. Ag-NPs showeda high level of antimicrobial activity against MDR-GNR. This is a rapid, low-cost, and eco-friendly technique. The results obtained using various physicochemical characterization techniques such as UV spectrophotometer, SEM, TEM, and XRD confirmed the presence of Ag-NPs. Further, fabricated Ag-NPs exhibited strong absorption maximum between 400 and 455 nm. The SEM and TEM images established the presence of spherical-shaped Ag-NPs that ranges in size from 20 and 50 nm. Among the test bacterial culture, the Ag-NPs exhibit efficient activity against the isolated MDR-GNR from suspected patients at BCH. The maximum Ag-NPs concentration achieved was between 75 and 100 μg with the zone of inhibition of about 15–17 mm. An important finding is that the release of Ag ions from Ag-NPs into the MDR bacteria could inhibit their growth effectively. These results suggest that the green synthesized Ag-NPs may serve as effective alternative antimicrobial agents against infections caused by MDR bacteria that pose a serious threat to public health. Moreover, this method will be very useful for producing more nanoparticles and it could be easily applied in the medical field as a biocide agent in hospitals, etc. The in vitro analysis confirmed that Ag-NPs serve as potential antimicrobial agents with high effectively. Finally, we recommended Ag-NPs as alternative broad-spectrum antimicrobial agents.

Declaration of Competing Interest

The authors declare that they have no known competing financial interests or personal relationships that could have appeared to influence the work reported in this paper.

Acknowledgments

This project was funded by King Abdulaziz City for Science and Technology (KACST), Kingdom of Saudi Arabia, Award Number 1-17-03-001-0030.

References

Al-Dhabi, N.A., Ghilan, A.-K.M., Arasu, M.V., 2018. Characterization of silver nanomaterials derived from marine Streptomyces sp. Al-Dhabi-87 and its in vitro application against multidrug resistant and extended-spectrum beta-lactamase. Clin. Pathogens Nanomater. 8 (5).

Al-Dhabi, N.A., Mohammed Ghilan, A.K., Esmail, G.A., Valan Arasu, M., Duraipandiyan, V., Ponmurugan, K., 2019. Bioactivity assessment of the Saudi Arabian Marine Streptomyces sp. Al-Dhabi-90, metabolic profiling and its in vitro inhibitory property against multidrug resistant and extended-spectrum beta-lactamase clinical bacterial pathogens. J. Infect Public Health 12, 549–556.

Al-Dhabi, N.A., Ghilan, A.K.M., Arasu, M.V., Duraipandiyan, V., 2019. Green biosynthesis of silver nanoparticles produced from marine Streptomyces sp. Al-Dhabi-89 and their potential applications against wound infection and drug resistant clinical pathogens. J. Photochem. Photobiol., B 111529.

Alfuraydi, A.A., Devanesan, S., Al-Ansari, M., AlSalhi, M.S., Ranjitsingh, A.J., 2019. Eco-friendly green synthesis of silver nanoparticles from the sesame oil cake and its potential anticancer and antimicrobial activities. J. Photochem. Photobiol. B. 192, 83–89.

Allaker, R.P., 2010. The use of nanoparticles to control oral biofilm formation. J. Dent. Res. 89 (11), 1175–1186.

AlSalhi, M.S., Devanesan, S., Alfuraydi, A.A., Vishnubalaji, R., Munusamy, M.A., Murugan, K., Nicoletti, M., Benelli, G., 2016. Green synthesis of silver nanoparticles using Pimpinella anisum seeds: antimicrobial activity and cytotoxicity on human neonatal skin stromal cells and colon cancer cells. Int. J. Nanomed. 11 (11), 4439–4449.

AlSalhi, M.S., Elangovan, K., Ranjitsingh, A.J.A., Murali, P., Devanesan, S., 2019. Synthesis of silver nanoparticles using plant derived 4-N-methyl benzoic acid and evaluation of antimicrobial, antioxidant and antitumor activity. Saudi J. Biol. Sci. 26, 970–978.

Arasu, M.V., Duraipandiyan, V., Ignacimuthu, S., 2013. Antibacterial and antifungal activities of polyketide metabolite from marine Streptomyces sp. AP-123 and its cytotoxic effect. Chemosphere 90 (2), 479–487.

Arasu, M.V., Thirumamagal, R., Srinivasan, M.P., Al-Dhabi, N.A., Ayeshamariam, A., Saravana Kumar, D., Punithavel, N., Jayachandran, M., 2017. Green chemical approach towards the synthesis of CeO2 doped with seashell and its bacterial applications intermediated with fruit extracts. J. Photochem. Photobiol., B 172, 50–60.

Arasu, M.V., Arokiyaraj, S., Viayaraghavan, P., Kumar, T.S.J., Duraipandiyan, V., Al-Dhabi, N.A., Kaviyarasu, K., 2019. One step green synthesis of larvicidal, and azo dye degrading antibacterial nanoparticles by response surface methodology. J. Photochem. Photobiol., B 190, 154–162.

Arokiyaraj, S., Saravanan, M., Badathala, V., 2015. Green synthesis of Silver nanoparticles using aqueous extract of Taraxacum officinale and its antimicrobial activity. South Indian J. Biol. Sci. 2, 115–118.

Azhaguraja, R., AlSalhi, M.S., Devanesan, S., 2017. Microwave-assisted synthesis of nickel oxide nanoparticles using coriandrum sativum leaf extract and their structural-magnetic catalytic properties. Materials 10, 460–472.

Bindhu, M.R., Umadevi, M., 2014. Surface plasmon resonance optical sensor and antibacterial activities of biosynthesized Ag-NPs. Spectrochim. Acta Part A-Mol. Biomol. Spectroscopy 121, 596–604.

Boovaragamoorthy, G.M., Anbazhagan, M., Piruthiviraj, P., Pugazhendhi, A., Kumar, S.S., Al-Dhabi, N.A., Ghilan, A.M., Arasu, M.V., Kaliannan, T., 2019. Clinically important microbial diversity and its antibiotic resistance pattern towards various drugs. J. Infection Public Health 19, 1876–10341.

Brown, A.N., Smith, K., Samuels, T.A., Lu, J.R., Obare, S.O., Scott, M.E., 2012. Nanoparticles functionalized with ampicillin destroy multiple-antibiotic-resistant isolates of Pseudomonas aeruginosa and Enterobacter aerogenes and methicillin-resistant Staphylococcus aureus. Appl. Environ. Microbiol. 78 (8), 2768–2774.

Chang, H.H., Cohen, T., Grad, Y.H., Hanage, W.P., O'Brien, T.F., 2015. Lipsitch M Origin and proliferation of multiple-drug resistance in bacterial pathogens. Microbiol. Mol. Biol. Rev. 79 (1), 101–116.

Devanesan, S., AlSalhi, M.S., Vishnubalaji, R., Alfuraydi, A.A., Alajez, N.M., Murugan, K., Sayed, S.R.M., Alfayez, M., Nicoletti, M., Benelli, G., 2017. Rapid biological synthesis of silver nanoparticles using plant seed extracts and their cytotoxicity on colorectal cancer cell lines. J. Clust. Sci. 28, 595–605.

Devanesan, S., AlSalhi, M.S., Balaji, R.V., Ranjitsingh, A.J.A., Ahamed, A., Alfuraydi, A. A., AlQahtani, F.Y., Aleanizy, F.S., Othman, A.H., 2018. Antimicrobial and cytotoxicity effects of synthesized silver nanoparticles from Punica granatum peel extract. Nanoscale Res. Lett. 13, 315.

Dibrov, P., Dzioba, J., Gosink, K.K., Hase, C.C., 2002. Chemiosmotic mechanism of antimicrobial activity of Ag+ in Vibrio cholerae. Antimicrob. Agents Chemother. 46 (8), 2668–26670.

Feng, Q.L., Chen, G.Q., Cui, F.Z., Kim, T.N., Kim, J.O., 2000. A mechanistic study of the antibacterial effect of silver ions on Escherichia coli and Staphylococcus aureus. J. Biomed. Mater. Res. 52 (4), 662–668.

Gopinath, V., MubarakAli, D., Priyadarshini, S., Priyadharsshini, N.M., Thajuddin, N., 2012. Velusamy P Biosynthesis of Ag-NPs from Tribulus terrestris and its antimicrobial activity: a novel biological approach. Colloids Surf. B-Biointerfaces 96, 69–74.

Gurusamy, S., Kulanthaisamy, M.R., Hari, D.G., Veleeswaran, A., Thulasinathan, B., Muthuramalingam, J.B., Balasubramani, R., Chang, S.W., Arasu, M.V., Al-Dhabi, N.A., Selvaraj, A., Alagarsamy, A., 2019. Environmental friendly synthesis of TiO2-ZnO nanocomposite catalyst and silver nanomaterials for the enhanced production of biodiesel from Ulva lactuca seaweed and potential antimicrobial properties against the microbial pathogens. J. Photochem. Photobiol., B 193, 118–130.

Ilavenil, S., Srigopalram, S., Park, H.S., Choi, K.C., 2015. Growth and metabolite profile of Pediococcus pentosaceus and Lactobacillus plantarum in different juice. South Indian J. Biol. Sci. 1, 1–6.

Jeeva, K., Thiyagarajan, M., Elangovan, V., Geetha, N., Venkatachalam, P., 2014. Caesalpinia coriaria leaf extracts mediated biosynthesis of metallic Ag-NPs and their antibacterial activity against clinically isolated pathogens. Ind. Crops Prod. 52, 714–720.

Kim, J.S., Kuk, E., Yu, K.N., Kim, J.H., Park, S.J., Lee, H.J., et al., 2007. Antimicrobial effects of Ag-NPs. Nanomed.-Nanotechnol. Biol. Med. 3 (1), 95–101.

Kumar, S., Singh, M., Halder, D., Mitra, A., 2014. Mechanistic study of antibacterial activity of biologically synthesized silver nanocolloids. Colloids Surf., A 449, 82–86.

Link-Gelles, R., Thomas, A., Lynfield, R., Petit, S., Schaffner, W., Harrison, L., et al., 2013. Geographic and temporal trends in antimicrobial nonsusceptibility in Streptococcus pneumoniae in the post-vaccine era in the United States. J. Infect. Dis. 208 (8), 1266–1273.

Murugan, K., Aruna, P., Panneerselvam, C., Madhiyazhagan, P., Paulpandi, M., Subramaniam, J., et al., 2016. Fighting arboviral diseases: low toxicity on mammalian cells, dengue growth inhibition (in vitro), and mosquitocidal activity of Centroceras clavulatum-synthesized Ag-NPs. Parasitol. Res. 115 (2), 651–662.

Panacek, A., Kvitek, L., Prucek, R., Kolar, M., Vecerova, R., Pizurova, N., et al., 2006. Silver colloid nanoparticles: synthesis, characterization, and their antibacterial activity. J. Phys. Chem. B 110 (33), 16248–16253.

Panda, K.K., Acharya, V.M.M., Krishnaveni, R., Padhi, B.K., Sarangi, S.N., Sahu, S.N., et al., 2011. In vitro biosynthesis and genotoxicity bioassay of Ag-NPs using plants. Toxicol. In Vitro 25 (5), 1097–1105.

Ping, Y., Zhang, J., Xing, T., Chen, G., Tao, R., Choo, K.H., 2018. Green synthesis of Ag-NPs using grape seed extract and their application for reductive catalysis of Direct Orange 26. J. Ind. Eng. Chem. 58, 74–79.

Priya Banerjee, M.S., Aniruddha, M., 2014. Papita D Leaf extract mediated green synthesis of Ag-NPs from widely available Indian plants: synthesis, characterization, antimicrobial property and toxicity analysis. Bioresour. Bioprocess. 1 (3), 71538–71541.

Rajkumari, J., Maria, Magdalane C., Siddhardha, B., Madhavan, J., Ramalingam, G., Al-Dhabi, N.A., Arasu, M.V., Ghilan, A.K.M., Duraipandiayan, V., Kaviyarasu, K., 2019b. Synthesis of titanium oxide nanoparticles using Aloe barbadensis mill and evaluation of its antibiofilm potential against Pseudomonas aeruginosa PAO1. J. Photochem. Photobiol., B 201, 111667.

Rajkumari, J., Maria, Magdalane C., Siddhardha, B., Madhavan, J., Ramalingam, G., Al-Dhabi, N.A., Arasu, M.V., Ghilan, A.K.M., Duraipandiayan, V., Kaviyarasu, K., 2019a. Synthesis of titanium oxide nanoparticles using Aloe barbadensis mill andevaluation of its antibiofilm potential against Pseudomonas aeruginosa PAO1. J. Photochem. Photobiol., B. https://doi.org/10.1016/j.jphotobiol.2019.111667.

Roca, I., Akova, M., Baquero, F., Carlet, J., Cavaleri, M., Coenen, S., 2015. The global threat of antimicrobial resistance: science for intervention. New Microbes New Infect. 8, 175.

Roopan, S.M., Priya, D.D., Shanavas, S., Acevedo, R., Al-Dhabi, N.A., Arasu, M.V., 2019. CuO/C nanocomposite: synthesis and optimization using sucrose as carbon source and its antifungal activity. Mater. Sci. Eng., C 101, 404–414.

Sondi, I., Salopek-Sondi, B., 2004. Ag-NPs as antimicrobial agent: a case study on E-coli as a model for Gram-negative bacteria. J. Colloid Interface Sci. 275 (1), 177–182.

Valsalam, S., Agastian, P., Arasu, M.V., Al-Dhabi, N.A., Ghilan, A.K.M., Kaviyarasu, K., Ravindran, B., Chang, S.W., Arokiyaraj, S., 2019a. Rapid biosynthesis and characterization of silver nanoparticles from the leaf extract of Tropaeolum majus L. and its enhanced in-vitro antibacterial, antifungal, antioxidant and anticancer properties. J. Photochem. Photobiol., B 191, 65–74.

Valsalam, S., Agastian, P., Esmail, G.A., Ghilan, A.K.M., Al-Dhabi, N.A., Arasu, M.V., 2019b.. Biosynthesis of silver and gold nanoparticles using Musa acuminata colla flower and its pharmaceutical activity against bacteria and anticancer efficacy. J. Photochem. Photobiol., B. https://doi.org/10.1016/j.jphotobiol.2019.111670.

Vijayaraghavan, K., Nalini, S.P.K., Prakash, N.U., Madhankumar, D., 2012. One step green synthesis of silver nano/microparticles using extracts of Trachyspermum ammi and Papaver somniferum. Colloids Surf. B-Biointerfaces 94, 114–117.